Weierstraß-Institut
für Angewandte Analysis und Stochastik
Leibniz-Institut im Forschungsverbund Berlin e. V.

Preprint ISSN 0946 – 8633

Homoclinic orbits in a two-patch predator-prey model with Preisach hysteresis operator

Alexander Pimenov[1], Dmitrii Rachinskii[2 3]

submitted: October 1, 2013

[1] Weierstrass Institute
Mohrenstr. 39
10117 Berlin
Germany
E-Mail: alexander.pimenov@wias-berlin.de

[2] Department of Mathematical Sciences
University of Texas at Dallas
800 W. Campbell Road
Richardson
TX 75080-3021
USA
E-Mail: Dmitry.Rachinskiy@utdallas.edu

[3] School of Mathematical Sciences
Department of Applied Mathematics
University College Cork
Cork
Ireland

No. 1849
Berlin 2013

2010 *Mathematics Subject Classification.* 47J40, 92D25, 37L15.

Key words and phrases. Robust homoclinic orbit, Preisach operator, operator-differential equations, predator-prey model.

A.P. acknowledges support of SFB 787 of the DFG under Grant B5. D.R. acknowledges support of the Russian Foundation for basic Research through grant 10-01-93112.

Edited by
Weierstraß-Institut für Angewandte Analysis und Stochastik (WIAS)
Leibniz-Institut im Forschungsverbund Berlin e. V.
Mohrenstraße 39
10117 Berlin
Germany

Fax: +49 30 20372-303
E-Mail: preprint@wias-berlin.de
World Wide Web: http://www.wias-berlin.de/

Abstract

Systems of operator-differential equations which hysteresis operators can have unstable equilibrium points with an open basin of attraction. In this paper, a numerical example of a robust homoclinic loop is presented for the first time in a population dynamics model with hysteretic response of prey to variations of predator. A mechanism creating this homoclinic trajectory is discussed.

1 Introduction

Hysteresis in relationships between various physical variables such as magnetic field and magnetization or mechanical stress and deformation can be modelled by a special class of non-smooth maps called hysteresis operators [6, 17, 24]. For example, constitutive equations of ferromagnetic, elastoplastic, piezoelectric, magnetostrictive and other smart materials have been modelled by the Preisach hysteresis operator and the Prandtl-Ishlinskii hysteresis operator [3, 9, 23, 25, 30]. Macroscopic models where such operator constitutive equations are coupled with differential equations of motion (or some form Maxwell's equations) [1, 2, 8, 12, 18–22, 29] present a class of infinite-dimensional dynamical systems whose dynamics may be substantially different from dynamics of smooth differential systems [4, 5, 10, 11, 15, 16]. As one example, a coupled system of differential equations

$$u' = f(u, v), \qquad x' = g(u, v) \tag{1}$$

and an operator equation

$$x(t) = (\mathcal{P}v)(t) \tag{2}$$

with the Preisach hysteresis operator $\mathcal{P}$ can have an unstable equilibrium which has an open basin of attraction (in the infinite-dimensional phase space of the system). Such equilibria, which have been called partially stable [26], can be compared to a saddle-node singular point of an ordinary differential system. Indeed, they simultaneously attract and repel many trajectories. However, unlike the classical saddle-node point, partially stable equilibria of system (1), (2) are robust.

The rigorous stability analysis presented in [26] for equilibria of equations (1), (2) has been illustrated with prototype examples of a few stable systems including an electronic circuit, a hydrological model, and a predator-prey dynamics model with safe and risky patches. Partially stable equilibria have been found numerically in an epidemiological model of a similar (but different) type [28]. The nature of partial stability suggests that if there is a homoclinic orbit attached to a partially stable equilibrium, then this homoclinic orbit is robust too. This may be interesting, for

example because a homoclinic orbit is associated with the so-called excitability phenomenon[1] when the system responds with a pulse to a small perturbation (which is localized in time); such a pulse is a manifestation of a large excursion in the phase space along the homoclinic orbit. Again, robust homoclinic orbits of operator-differential systems contrast with generic homoclinic orbits of smooth differential systems, as the latter are removable by arbitrarily small perturbations (a homoclinic bifurcation to a saddle or saddle node).

In this paper, we give a numerical evidence that a robust homoclinic orbit exists in a population dynamics model where the prey switches between two modes of behaviour, risky and safe, in response to varying abundance of predator. In the safe state, the prey enjoys lower killing rate by the predator at the price of increased competition rate. The Preisach operator defines how the rate of exchange between the risky and safe prey populations responds to variations of the predator number. Effectively, it introduces memory in the switching strategy (rule) of the prey.

The homoclinic orbit results from a combination of local dynamics near a partially stable equilibrium and global dynamics which drives those trajectories that leave a small neighbourhood of this equilibrium back to it. The homoclinic trajectory has two parts separated by a point where the predator population achieves maximum. The trajectory satisfies a different system of ordinary differential equations on each of these two parts. Both ordinary differential systems have the same equilibrium which is unstable for the first system and stable for the second system. Moreover, the switching point belongs to the basin of attraction of the equilibrium of the second system.

A rigorous proof of the existence of a stable homoclinic orbit near the observed numerical solution is beyond the scope of this paper and will be the subject of future work. We note that when stability is analysed, one has to consider not only perturbations of phase variables (predator and two prey populations), but also perturbations of the infinite-dimensional memory state of the Preisach operator [27].

The system and a brief description of the Preisach hysteresis operator are presented in the next section, which is followed by the sections presenting numerical results, some related analysis and discussion. The derivation of the model is contained in the Appendix.

[1]The term “Excitability” was originally coined in the analysis of the action potential of the axon of the giant Atlantic squid [14]. It is now commonly used to describe any stable dynamical system that exhibits pulses when perturbed above a certain threshold level.

2 Excitable behaviour in a predator-prey system

2.1 The model

In this work, we consider a two-patch extension of the model proposed in [13], which has non-trivial dynamical properties such as multiple stable equilibria:

$$\dot{u}_R = a_R(u_R) - f_R(u_R)g(v) + h_R(t)u_S - h_S(t)u_R, \tag{3}$$

$$\dot{u}_S = a_S(u_S) - f_S(u_S)g(v) - h_R(t)u_S + h_S(t)u_R, \tag{4}$$

$$\dot{v} = \sigma(f_R(u_R) + f_S(u_S))g(v) - c(v). \tag{5}$$

Here dot denotes differentiation with respect to time; u_R is the number of prey in the Risky patch; u_S is the number of prey in the Safe patch; v is the number of predator; the terms

$$a_{R/S}(u) = \rho u - \lambda_{R/S}u^2$$

describe logistic growth of the prey inside the patches with birth rate ρ and competition rates $\lambda_{R/S}$;

$$f_{R/S}(u) = \frac{\omega_{R/S}u}{\phi + u}$$

is the Holling type II functional response;

$$g(v) = \frac{v}{1 + \beta v}$$

is the predator interference; σ is the efficiency of conversion of food to growth; and, the term

$$c(v) = \gamma v$$

describes death of the predator with the death rate γ. The attack rates for Risky and Safe patches satisfy $\omega_R > \omega_S \geq 0$, and we assume that the prey pays a price for choosing the safe patch with higher competition, $\lambda_S > \lambda_R > 0$. A similar two-patch system was considered, e.g., in [7].

There is flow of prey from the Risky to Safe patch, $h_S(t)u_R$, and in the opposite direction, $h_R(t)u_S$. The simplest choice of the flow rate $h_S(t)$ in one direction is a constant, $h_S(t) = k_{S0}$. In terms of the differentials, $du_S = k_{S0}u_R dt$. Another option is to implement a flow in reaction to the change of some function $p(v)$ of the predator number by assuming that $du_S = k_S u_R dp(v)$. Combining these two formulas results in

$$h_S(t) = \left(k_{S0} + k_S\frac{dp}{dv}\dot{v}\right)^+,$$

where we ensure that the flow is positive by applying the function $x^+ = \max\{x, 0\}$. Now, equation (5) can be used to substitute for $\dot{v}$. Similarly, $h_R(t) = \left(k_{R0} - k_R\frac{dp}{dv}\dot{v}\right)^+$.

In this paper, we are interested in the situation when the reaction of prey to variations of the predator population is hysteretic. Namely, we assume that

$$du_S = k_S u_R d(\mathcal{P}[\eta_0]v), \quad du_R = -k_R u_S d(\mathcal{P}[\eta_0]v),$$

where $\mathcal{P}$ is the Preisach operator with the initial state η_0 [5], and the total flow to the Risky and Safe patch is defined by

$$h_S(t) = \left(k_{S0} + k_S \frac{d}{dt}(\mathcal{P}[\eta_0]v)(t)\right)^+, \; h_R(t) = \left(k_{R0} - k_R \frac{d}{dt}(\mathcal{P}[\eta_0]v)(t)\right)^+, \quad (6)$$

respectively. The Preisach operator appears from the assumption that the prey does not respond immediately to a change of the trend in predator dynamics (i.e., the change of the sign of $\dot{v}$). The change of the rate of flows between the patches is delayed until the abundance of predator drops/increases from its extremum value by a certain sufficiently large amount. More detailed derivation of the model is presented in the Appendix.

The Preisach operator is defined by

$$(\mathcal{P}[\eta_0]v)(t) = \int_0^\infty \int_0^{\alpha_S} \mu(\alpha_R, \alpha_S)(R_{\alpha_R,\alpha_S}[\eta_0(\alpha_R, \alpha_S)]v)(t)\, d\alpha_R d\alpha_S, \quad (7)$$

where $v(t), t \geq t_0$ is the input; the function $\eta_0 = \eta_0(\alpha_R, \alpha_S)$ which takes values 0 and 1 is the initial state function; $\mu(\alpha_R, \alpha_S)$ is an integrable density function; and R_{α_R,α_S} is the non-ideal relay operator with thresholds α_R, α_S satisfying $0 < \alpha_R \leq \alpha_S$:

$$(R_{\alpha_R,\alpha_S}[\eta_0]v)(t) = \begin{cases} 0 & \text{if} \quad v(\tau) \leq \alpha_R \text{ for some } \tau \in [t_0, t] \\ & \quad \text{and } v(s) < \alpha_S \text{ for all } s \in [\tau, t]; \\ 1 & \text{if} \quad v(\tau) \geq \alpha_S \text{ for some } \tau \in [t_0, t] \\ & \quad \text{and } v(s) > \alpha_R \text{ for all } s \in [\tau, t]; \\ \eta_0(\alpha_R, \alpha_S) & \text{if} \quad \alpha_R < v(\tau) < \alpha_S \text{ for all } \tau \in [t_0, t]. \end{cases} \quad (8)$$

It is convenient to represent states (8) of the relays graphically in the domain $0 \leq \alpha_R \leq \alpha_S$ of the plane (α_R, α_S). It suffices to consider the situation when this domain is divided into two parts by a staircase polyline $\Omega = \Omega(t)$ with the relays in state 1 below (to the left) of this line and in state 0 above (to the right) of this line, see Fig. 1 (left). The polyline Ω can have either finite or infinite number of horizontal and vertical links, but in the latter case the only accumulation point of the corners is the right end of the polyline. The right end is the point $\alpha_R = \alpha_S = v(t)$ at any moment $t \geq t_0$ [17].

Formula (8) defines how the staircase polyline $\Omega(t)$ dividing the domains where $R_{\alpha_R,\alpha_S} = 0$ and $R_{\alpha_R,\alpha_S} = 1$ changes over time in response to variations of a continuous non-negative input $v(t)$. For example, suppose that Ω at $t = t_0$ is the horizontal segment $\alpha_S = v(t_0)$, $0 \leq \alpha_R \leq v(t_0)$ (see Fig. 1, right). If $v(t)$ monotonically decreases on an interval $t \in [t_0, t_1]$, then Ω acquires the vertical link $\alpha_R = v(t)$, $v(t) \leq \alpha_S \leq v(t_0)$ as shown in Fig. 2, left. If thereafter the input monotonically increases for $t \in [t_1, t_3]$, then a new horizontal link $\alpha_S = v(t)$, $v(t_1) \leq \alpha_R \leq v(t)$ appears (see Fig. 2, right). However, if the input reaches its initial value $v(t_0)$ at some moment t_*, then Ω becomes a horizontal segment again, as at the initial moment (see Fig. 1, right). If the input increases further, $\Omega(t)$ remains horizontal until the input reaches a maximum point $v(t_3)$ (at which a vertical link will be created with the subsequent decrease of the input to $v(t_4)$, see Fig. 3). In this manner, vertical and horizontal links can be created and deleted in response to variations of the input $v(t)$. An input with many local

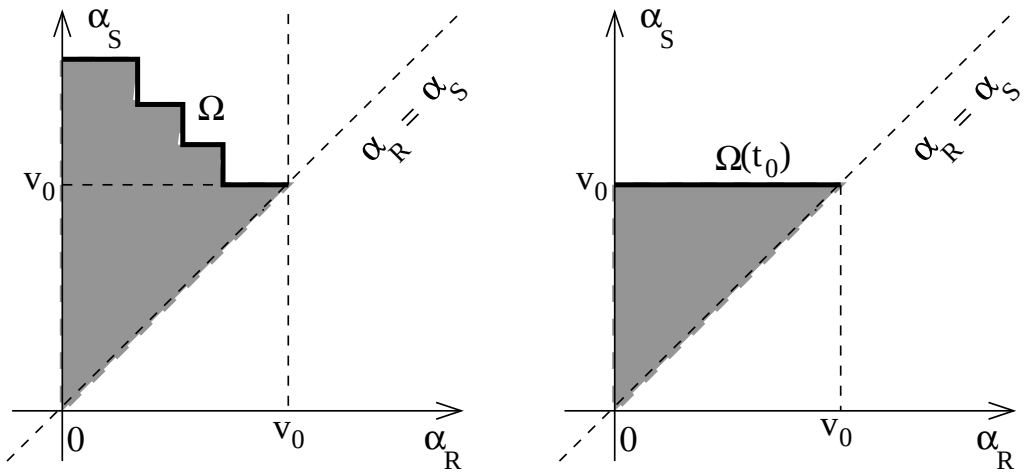

Figure 1: The domain $0 \le \alpha_R \le \alpha_S$ of the plane (α_R, α_S) is divided into two parts by a staircase polyline $\Omega = \Omega(t)$ with the relays in state 1 below (to the left) of this line (grey colour) and in state 0 above (to the right) of this line (white colour). Here $v_0 = v(t_0)$. In the right figure $\Omega(t_0)$ is the horizontal segment $\alpha_S = v(t_0)$, $0 \le \alpha_R \le v(t_0)$.

maximum and minimum points can create a staircase line Ω with multiple links. We refer to [5] for more details. The polyline $\Omega(t)$ is often referred to as the state of the Preisach operator.

In equations (3)-(6), the derivative of the output of the Preisach operator is used. For the evaluation of this derivative, the most right link $\Omega_e = \Omega_e(t)$ which is attached to the right end point $\alpha_R = \alpha_S = v(t)$ of the staircase polyline $\Omega(t)$ is of importance, see Fig. 4, left (if Ω has infinitely many links, then $\Omega_e = \emptyset$). Denote by $(v_m, v), (v, v_M)$ the end points of the segment Ω_e, where $v_m = v$ if Ω_e is a vertical segment and $v_M = v$ if Ω_e is horizontal. If $v = v(t)$ increases, then the time derivative of the output of the Preisach operator satisfies

$$\frac{d(\mathcal{P}[\eta_0]v)}{dt} = \dot{v} H(v, v_m) \quad \text{with} \quad H(v, v_m) = \int_{v_m}^{v} \mu(\alpha_R, v)\, d\alpha_R. \tag{9}$$

If v decreases, then

$$\frac{d(\mathcal{P}[\eta_0]v)}{dt} = \dot{v} V(v, v_M) \quad \text{with} \quad V(v, v_M) = \int_{v}^{v_M} \mu(v, \alpha_S)\, d\alpha_S. \tag{10}$$

In the case of increasing v, substituting formula (9) in equations (6), we see that the flows between the patches are equal to

$$h_S(t) = (k_{S0} + k_S \dot{v} H(v, v_m))^+, \quad h_R(t) = (k_{R0} - k_R \dot{v} H(v, v_m))^+, \tag{11}$$

where $\dot{v}$ can be replaced with the right hand side of equation (5). Similarly, when v decreases,

$$h_S(t) = (k_{S0} + k_S \dot{v} V(v, v_M))^+, \quad h_R(t) = (k_{R0} - k_R \dot{v} V(v, v_M))^+. \tag{12}$$

Equilibria of system (3)-(8) can be found from the algebraic system, which is obtained by setting the derivatives of all the variables including $d/dt(\mathcal{P}[\eta_0]v)$ in (3)-(8) to zero. In the next section,

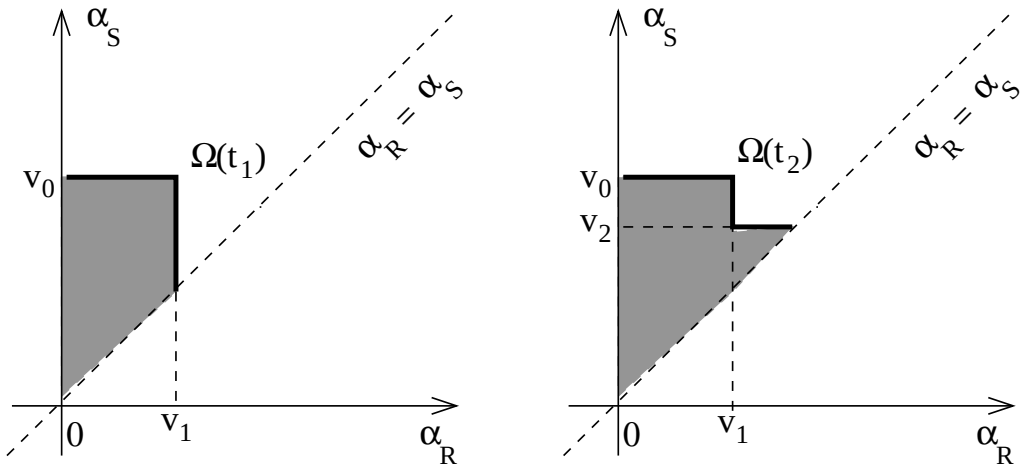

Figure 2: Evolution of the staircase state $\Omega = \Omega(t)$ from the initial state $\Omega(t_0)$ shown in Fig. 1 (right) in response to an input $v(t)$, which monotonically decreases on an interval $t \in [t_0, t_1]$. For $t_0 < t \leq t_1$ the line Ω consists of two segments. Left panel presents the state at the moment t_1: the vertical link $\alpha_R = v(t_1)$, $v(t_1) \leq \alpha_S \leq v(t_0)$ connects to the horizontal link, which is a part of the segment $\Omega(t_0)$ shown in Fig. 1 (right). After the moment t_1, the input $v(t)$ monotonically increases for $t \in [t_1, t_2]$. We assume $v(t_1) < v(t_2) < v(t_0)$. In this case, the state Ω has three links for $t_1 < t \leq t_2$ as shown on the right panel for the moment $t = t_2$. The left horizontal link and the vertical link of the line $\Omega(t_2)$ are parts of the staircase $\Omega(t_1)$ presented on the left panel. The extra right horizontal link is $\alpha_S = v(t_2)$, $v(t_1) \leq \alpha_R \leq v(t_2)$. Here $v_i = v(t_i)$.

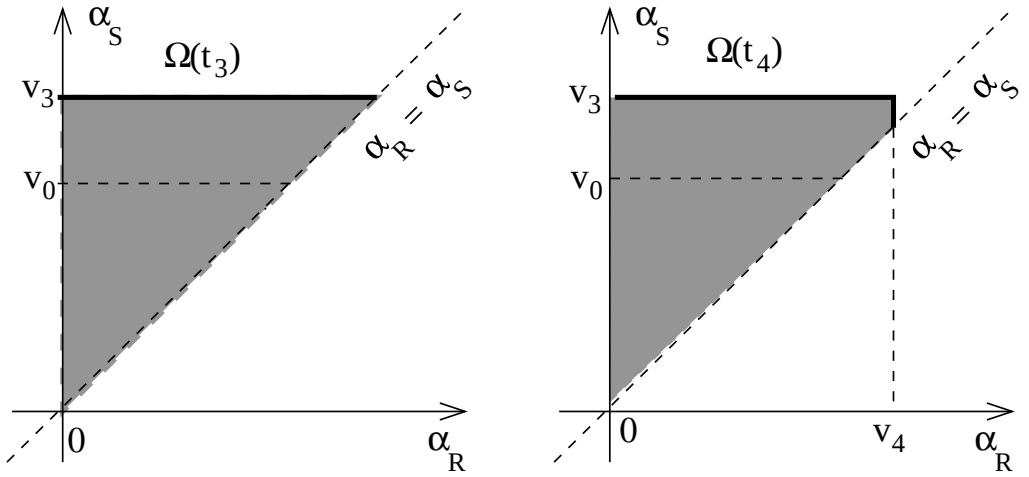

Figure 3: Evolution of $\Omega(t)$ from the state $\Omega(t_2)$ shown in Fig. 2 (right). The input $v(t)$ increases on an interval $[t_2, t_3]$ from the value $v(t_2) = v_2 < v_0$ to a value $v(t_3) = v_3 > v_0$. At the moment t_* when the input reaches the value v_0, the state Ω becomes the horizontal segment (as a matter of fact, $\Omega(t_*) = \Omega(t_0)$) and remains the horizontal segment $\alpha_S = v(t)$, $0 \leq \alpha_R \leq v(t)$ for all $t_* \leq t \leq t_3$ as shown on the left panel. The input is assumed to decrease again after the moment t_3. The corresponding state Ω presented on the right panel for a moment $t_4 > t_3$ is similar to the staircase in Fig. 2 (left).

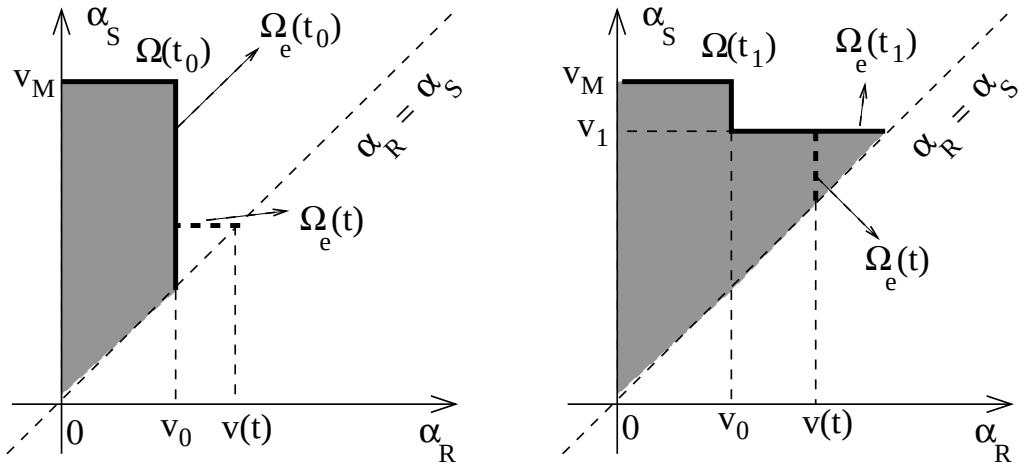

Figure 4: Evolution of the staircase state $\Omega(t)$ for the numerical example of a homoclinic trajectory (see Figs. 5, 6); $\Omega_e(t)$ is the lower right segment of this staircase state with the end-point $\alpha_R = \alpha_S = v(t)$ on the bisector. The initial state $\Omega(t_0)$ (solid line on the left panel) consists of a horizontal segment and the vertical segment $\Omega_e(t_0)$. During the time interval $(t_0, t_1]$ when the input $v(t)$ increases, $\Omega(t)$ has three segments, the segment $\Omega_e(t)$ is horizontal (solid dashed line). The right panel shows the state $\Omega(t_1)$ (solid line) at the moment when the input achieves its maximum $v(t_1) = v_1$. After this moment, the input decreases, $\Omega(t)$ consists of four segments, and the segment $\Omega_e(t)$ is vertical (solid dashed line).

we present a numerical example of the homoclinic trajectory (see Fig. 5, 6) which is obtained as follows. First, an equilibrium (u_R^*, u_S^*, v^*) of system (3)-(8) is identified, and we choose an initial state $\Omega(t_0)$ of the Preisach operator at the equilibrium with a sufficiently long vertical segment $\Omega_e(t_0)$ (see Fig. 4, left). Next, we consider an (arbitrarily) small perturbation of initial values $(u_R(t_0), u_S(t_0), v(t_0))$ from the equilibrium with $v(t_0) = v^*$ such that $\dot{v}(t_0) > 0$. Hence, initially, $v(t)$ increases, therefore the trajectory of (3)-(8) can be obtained as a solution of the system of ordinary differential equations (3)-(5), (11) with $v_m = v(t_0)$. The choice of parameters ensures that the point (u_R^*, u_S^*, v^*) is an equilibrium of saddle type for this ordinary differential system, hence the solution deviates from the equilibrium. Now, we extend the solution (with the increasing component $v(t)$) to a point where it hits the surface $\dot{v} = 0$ at a moment t_1 (see Fig. 4, right). After this moment, $v(t)$ decreases, hence the next segment of the trajectory of system (3)-(8) becomes a solution of ordinary differential system (3)-(5), (12) with $v_M = v(t_1)$. Our choice of parameters ensures that (u_R^*, u_S^*, v^*) is a stable node for this ordinary differential system and that the switching point $(u_R(t_1), u_S(t_1), v(t_1))$ belongs to the basin of attraction of this node. Therefore the trajectory converges back to the equilibrium. In particular, the state $\Omega(t)$ of the Preisach operator converges to its initial state $\Omega(t_0)$ as $t \to \infty$. Summarizing, the homoclinic orbit of system (3)-(8) has two parts, satisfying two different ordinary differential systems which have the same equilibrium. This equilibrium is a saddle for the first system and a node for the second system.

2.2 Numerical results

Using a criterion for existence of multiple positive equilibria [13], we set $\rho = 1.35$, $\phi = 0.1$, $\beta = 1.2$, $\gamma = 0.5$, $\omega_R = 2$, $\omega_S = 0$ (no predators in the safe patch), $k_{S0} = 0.01$, $k_{R0} = 0.001$, $\lambda_S = 0.1$, $\lambda_R = 0.01$ to ensure that system (3)-(8) has three positive equilibrium points

$$(u_R^*, u_S^*, v^*) = (0.206995, 13.4915, 0.2904365), \tag{13}$$

$$(u_R^\dagger, u_S^\dagger, v^\dagger) = (0.306704, 13.4923, 0.4235345), \tag{14}$$

$$(u_R^\ddagger, u_S^\ddagger, v^\ddagger) = (133.387, 14.4153, 0.8373). \tag{15}$$

If $k_R = k_S = 0$ (the exchange terms (6) do not have a component with the Preisach operator), then equilibria (13), (14), (15) of the system of ordinary differential equations (3)-(5) have the eigenvalues $(-1.35, 0.084, 0.67)$, $(-1.35, -0.062, 0.89)$, and $(-1.53, -1.33, -0.25)$, respectively. That is, the first and the second equilibria are saddles and the third equilibrium is a stable node.

When the hysteresis terms are present, we give a numerical evidence that equilibrium (13) can become partially stable and can have a homoclinic orbit attached to it. We set $k_R = 0.1k_S$ and define the density function of the Preisach operator (7) by the formula

$$\mu(\alpha_R, \alpha_S) = \frac{\exp(-900(\alpha_R - 0.2904365)^2)}{0.042},$$

in the triangle $0 \le \alpha_R \le \alpha_S \le 1$ with $\mu = 0$ outside this triangle. The maximum of this Gaussian density distribution corresponds to the equilibrium value v^* of the predator. The integral of μ over the whole half plane $\alpha_S \ge \alpha_R$ is normalized to 1.

As the initial state of the Preisach operator we choose the polyline $\Omega(t_0)$ which has two links: a vertical link $\Omega_e(t_0) = \{\alpha_R = v^*, v^* \le \alpha_S \le v_M\}$ and a horizontal link $\{\alpha_S = v_M, 0 \le \alpha_R \le v^*\}$ with $v_M = 1$ (see Fig. 4, left). The initial populations are $v(t_0) = v^*, u_R(t_0) \approx u_R^* + 10^{-5}, u_S(t_0) = u_S^*$. For $k_S = 1$, the trajectory of system (3)-(8) starting from these initial values, which are close to equilibrium (13), converges to equilibrium (15) (see Fig. 5, dashed line). The component $v(t)$ of this trajectory monotonically increases, hence this trajectory is simultaneously a solution of the ordinary differential system (3)-(5), (11) with $v_m = v(t_0) = v^*$, for which equilibrium (13) is a saddle with eigenvalues

$$(-1.34931, 0.0839766, 0.665618) \tag{16}$$

and equilibrium (15) is a stable node.

Increasing the parameter k_S to the value $k_S = 5.035$, we observe that the trajectory Γ of system (3)-(8) with the same initial values hits the surface $\dot{v} = 0$ at $v(t_1) = 0.3707$. Again, on the interval $[t_0, t_1]$ this trajectory is a solution of the ordinary differential system (3)-(5), (11) (with $v_m = v(t_0) = v^*$), for which the saddle equilibrium (13) has the same eigenvalues (16). However, after the moment t_1 the component $v(t)$ of the trajectory Γ of system (3)-(8) decreases and we show numerically that the trajectory Γ is attracted asymptotically towards the same equilibrium (13) near which it started (see Fig. 5, solid line). The part of Γ corresponding to $t > t_1$ is a solution of the ordinary differential system (3)-(5), (12) (with $v_M = v(t_1)$), for which the

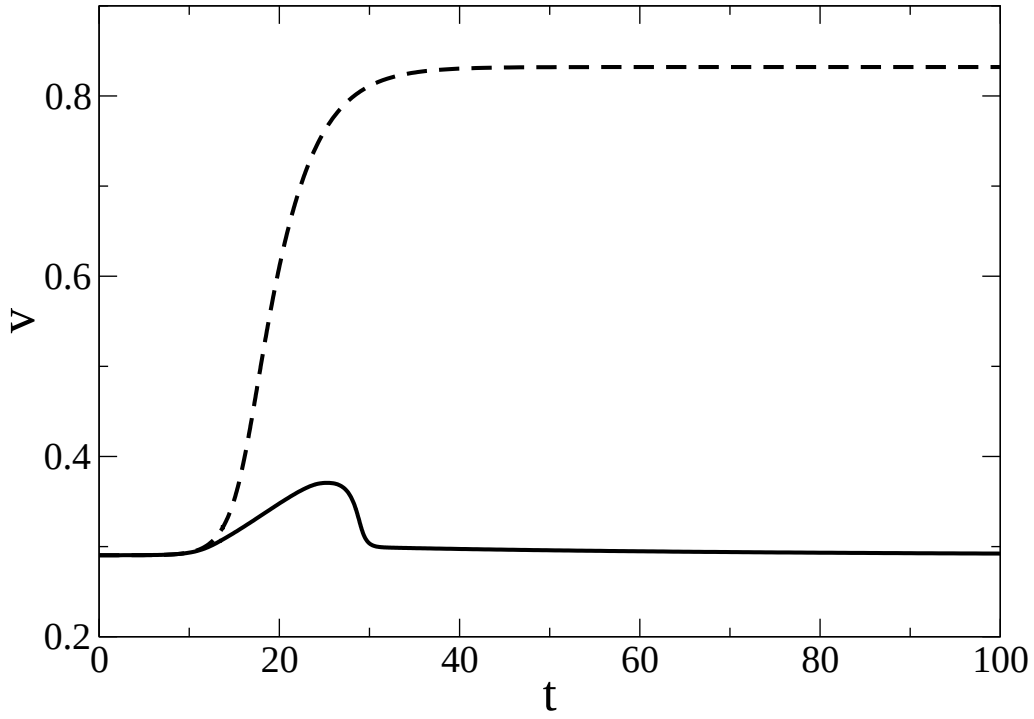

Figure 5: Time series of the predator for two trajectories obtained by a small perturbation of initial date from the equilibrium $(0.206995, 13.4915, 0.2904365)$ (equilibrium (13)) for $k_S = 1$ (dashed line) and $k_S = 5.035$ (solid line).

equilibrium (13) is a stable node with the eigenvalues $(-2.66012, -1.34664, -0.0210543)$. Hence, the above results of numerical simulation of system (3)-(8) complemented by the local stability analysis of the associated ordinary differential systems suggest that we have demonstrated a robust homoclinic behaviour in system (3)-(8) with the Preisach hysteresis operator (see Fig. 6) by following the plan outlined in the previous subsection.

Increasing k_S further above the value $k_S = 5.1$, we observe numerically more complicated behaviour of trajectories of system (3)-(8) such as oscillating transients before convergence to an equilibrium, which for higher values of k_S give rise to a periodic regime (Hopf bifurcation scenario). However, discussion of these dynamics is beyond the scope of the paper.

3 Conclusion

We have proposed a predator-prey model, where the prey can prefer to stay in one of two patches: the Safe patch, where the prey enjoys lower killing rate by the predator at the price of increased competition rate; and the Risky patch. The rate of flow between the patches is assumed to depend on the number of predator; this dependence is described by a hysteresis operator. A mechanism which can produce a homoclinic orbit attached to a partially stable equilibrium of a differential system with hysteresis nonlinearity has been discussed. Using the two-patch predator-prey system as an example, we have demonstrated numerically for the first

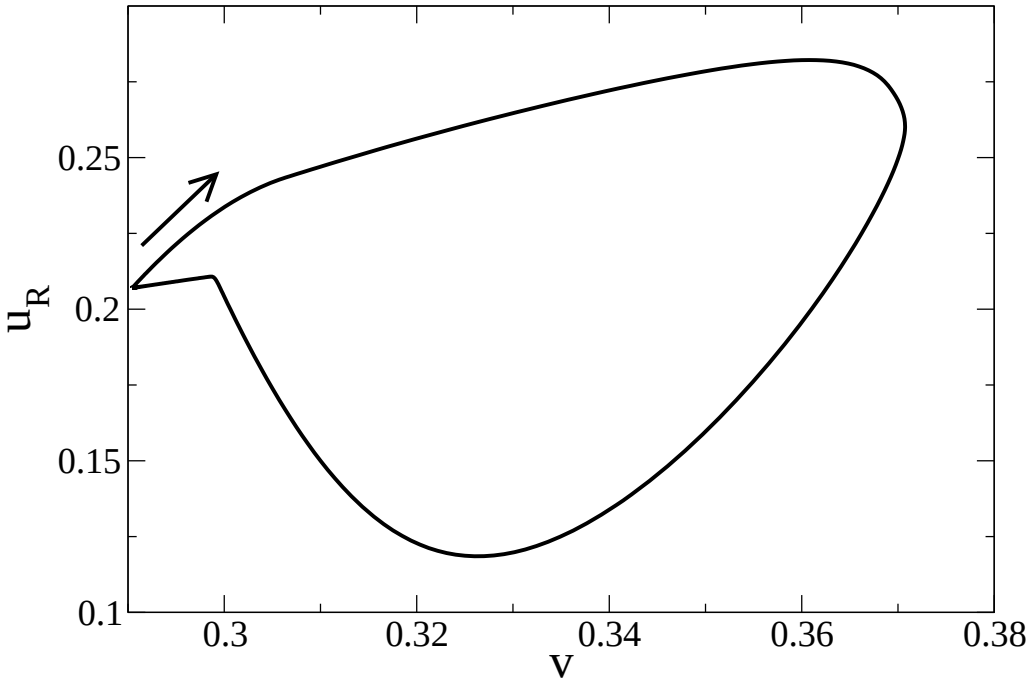

Figure 6: Homoclinic loop for $k_S = 5.035$. The orbit starts from the leftmost point and continues in the direction of the arrow.

time a homoclinic orbit, which persists for a substantial range of parameter values (a robust homocline).

4 Appendix

We consider a two-layer-type environment, where the top layer corresponds to risky conditions, and the bottom layer corresponds to safe conditions (such as sandy bottom of a natural water reservoir, which can serve as a refuge for some fish species). We assume that the predator species move freely around the whole environment and there is a flow of prey species between Safe and Risky layers. Environment is composed of equally-sized cells such that each cell has both layers (patches) in the same proportion, and the prey moves freely between the cells. Then a change in the number of species in each patch can be represented symbolically in terms of

differentials as follows:

Population dynamics	$du_R = X_R(u_R, v)dt;$ $du_S = X_S(u_S, v)dt;$ $dv = Y(u_R, u_S, v)dt;$
Constant flow from Risky to Safe patch	$du_S = -du_R = k_{S0}u_R dt;$
Constant flow from Safe to Risky patch	$du_S = -du_R = -k_{R0}u_S dt;$
Flow to Safe patch in reaction to v	$du_S = -du_R = k_S u_R d(F_r[\eta_0]v);$
Flow to Risky patch in reaction to v	$du_S = -du_R = k_R u_S d(F_r[\eta_0]v).$

Here

$$w(t) = (F_r[s_0]v)(t), \qquad t \geq t_0 \tag{17}$$

is the so-called *play* operator [17] of width $2r \geq 0$ with the initial state $s_0 \in [-r, r]$, which is defined on the class of all piecewise monotone continuous inputs $v = v(t)$ by the recurrent relationships $w(t_0) = v(t_0) - s_0$ and $w(t) = \phi_r(v(t), w(t_{i-1}))$, $t \in [t_{i-1}, t_i]$, $i \geq 1$, where

$$\phi_r(v, w) = \max\{v - r, \min\{v + r, w\}\}$$

and $[t_{i-1}, t_i]$ are intervals of monotonicity of the input v. The play operator admits a continuous extension $v(t) \mapsto w(t) = (F_r[s_0]v)(t)$ to the space of continuous functions with the supremum norm; furthermore, the extended play operator has a continuous restriction to the the space of absolutely continuous functions with $W^{1,1}$-norm [6].

According to the definition of the play operator, the intensity of exchange of prey between the patches responds to the predator abundance $v(t)$ as follows. If v monotonically increases (and $s_0 = r$) or v monotonically decreases (and $s_0 = -r$), then increments of the rate (17) of flow of prey between the patches are proportional to increments of the predator abundance, $dw = dv$. If $v(t)$ reaches a local maximum at $v(t_1) = v_M$ (or a local minimum at $v(t_2) = v_m$), then there is a window of inactivity such that $dw/dt = 0$ while v remains between $v_M - 2r$ and v_M (between v_m and $v_m + 2r$, respectively). After $v(t)$ has reached either end of the inactivity window, the increments of w and v become proportional again, $dw = dv$, until v reaches another extremum value and another window of inactivity occurs. In other words, if the trend of predator abundance reverses, the prey hesitates until either the new trend changes the number of predator by $2r$ or until the old trend resumes and the number of predator recovers. Then the prey acts according to the trend of the predator again.

Now, we allow for heterogeneity of the cells of environment by assuming that the width of the inactivity window $2r$ is specific to a cell and has a distribution $\psi(r)$ over all cells. Assuming that the free movement of prey between the cells is much faster than all other processes, we arrive at the averaged formulas for flows between the Safe and Risky patches in response to $v(t)$:

$$du_S = -du_R = k_S u_R d(P[s_0]v), \quad du_S = -du_R = k_R u_S d(P[s_0]v),$$

where

$$(P[s_0]v)(t) = \int_0^\infty \psi(r)(F_r[s_0(r)]v)(t)ds \tag{18}$$

is the Prandtl-Ishlinskii hysteresis operator with the initial state $s_0 = s_0(r)$ [17]. Furthermore, we allow a more general form of the expression for differentials of the exchange flows by replacing the Prandtl-Ishlinskii operator with the Preisach operator. According to P. Krejčı's formula, the Preisach operator has an equivalent representation

$$(\mathcal{P}[\eta_0]v)(t) = \int_0^\infty \phi(r, (F_r[s_0(r)]v)(t))dr.$$

For $\phi(r, u) = \psi(r)u$, this formula reduces to (18).

Combining the population terms with the hysteretic exchange terms and the constant flows, we obtain the system

$$\begin{gathered}\dot{u}_R = X_R(u_R, v) + h_R(t)u_S - h_S(t)u_R,\\ \dot{u}_S = X_S(u_S, v) - h_R(t)u_S + h_S(t)u_R,\\ \dot{v} = Y(u_R, u_S, v)\end{gathered}$$

with h_S, h_R defined by formulas (6). System (3)-(8) is obtained by choosing specific population terms $X_{R/S}, Y$ in accordance with assumptions presented in Section 2.

References

[1] B. Appelbe, D. Flynn, H. McNamara, P. O'Kane, A. Pimenov, A. Pokrovskii, D. Rachinskii, and A. Zhezherun. Rate-independent hysteresis in terrestrial hydrology. *Control Systems Magazine, IEEE*, 29(1):44–69, 2009. DOI 10.1109/MCS.2008.930923.

[2] B. Appelbe, D. Rachinskii, and A. Zhezherun. Hopf bifurcation in a van der Pol type oscillator with magnetic hysteresis. *Physica B: Condensed Matter*, 403(2):301–304, 2008. DOI 10.1016/j.physb.2007.08.034.

[3] Giorgio Bertotti, Isaak Mayergoyz, and Claudio Serpico. Nonlinear magnetization dynamics. Switching and relaxation phenomena. In Isaak Mayergoyz and Giorgio Bertotti, editors, *The Science of Hysteresis*, volume II, chapter VI, pages 435–565. Elsevier, Academic Press, 2005. Zbl 1148.78001, MR2307930.

[4] M. Brokate, A. Pokrovskii, and D. Rachinskii. Asymptotic stability of continuum sets of periodic solutions to systems with hysteresis. *Journal of Differential Equations*, 319(1):94–109, 2006. Zbl 1111.34035, MR2217849, DOI 10.1016/j.jmaa.2006.02.060.

[5] M. Brokate, A.V. Pokrovskii, D.I. Rachinskii, and O. Rasskazov. Differential equations with hysteresis via a canonical example. In Isaak Mayergoyz and Giorgio Bertotti, editors, *The Science of Hysteresis*, volume I, chapter II, pages 125–291. Elsevier, Academic Press, 2005. Zbl 1142.34026, MR2307929.

[6] M. Brokate and J. Sprekels. *Hysteresis and Phase Transitions*. Springer, Berlin, 1996. Zbl 0951.74002, MR1411908.

[7] Giovanna Chiorino, Pierre Auger, Jean-Luc Chassé, and Sandrine Charles. Behavioral choices based on patch selection: a model using aggregation methods. *Mathematical Biosciences*, 157:189–216, 1999. MR1686474, DOI 10.1016/S0025-5564(98)10082-2.

[8] R. Cross, H. McNamara, A. Pokrovskii, and D. Rachinskii. A new paradigm for modelling hysteresis in macroeconomic flows. *Physica B: Condensed Matter*, 403(2):231–236, 2008. DOI 10.1016/j.physb.2007.08.017.

[9] Daniele Davino, Pavel Krejčí, and Ciro Visone. Fully coupled modeling of magneto-mechanical hysteresis through 'thermodynamic' compatibility. *Smart Materials and Structures*, 22(9):095009, 2013. DOI 10.1088/0964-1726/22/9/095009.

[10] P. Diamond, N. Kuznetsov, and D. Rachinskii. On the Hopf bifurcation in control systems with a bounded nonlinearity asymptotically homogeneous at infinity. *Journal of Differential Equations*, 175(1):1–26, 2001. Zbl 0984.34029, MR1849221, DOI 10.1006/jdeq.2000.3916.

[11] P. Diamond, D. Rachinskii, and M. Yumagulov. Stability of large cycles in a nonsmooth problem with Hopf bifurcation at infinity. *Nonlinear Analysis: Theory, Methods & Applications*, 42(6):1017–1031, 2000. Zbl 0963.34034, MR1780452, DOI 10.1016/S0362-546X(99)00162-5.

[12] M. Eleuteri, J. Kopfova, and P. Krejčí. Magnetohydrodynamic flow with hysteresis. *SIAM Journal on Mathematical Analysis (SIMA)*, 41(2):435–464, 2009. Zbl 05696710, MR2507458, DOI 10.1137/080718383.

[13] Gary W. Harrison. Multiple stable equilibria in a predator-prey system. *Bulletin of Mathematical Biology*, 48:137–148, 1986. Zbl 0585.92023, MR0845634, DOI 10.1007/BF02460019.

[14] A. L. Hodgkin and A. F. Huxley. A quantitative description of membrane current and its application to conduction and excitation in nerve. *J. Physiol.*, 117:500, 1952. DOI 10.1007/BF02459568.

[15] A. Krasnosel'skii and D. Rachinskii. On a bifurcation governed by hysteresis nonlinearity. *Nonlinear Differential Equations and Applications (NoDEA)*, 9(1):93–115, 2002. Zbl 1013.34036, MR1891697, DOI 10.1007/s00030-002-8120-2.

[16] A.M. Krasnosel'skii and D. I. Rachinskii. On the continua of cycles in systems with hysteresis. *DOKLADY MATHEMATICS C/C OF DOKLADY-AKADEMIIA NAUK*, 63(3):339–344, 2001. Zbl 1052.34052, MR1863745.

[17] M. A. Krasnosel'skii and A. V. Pokrovskii. *Systems with Hysteresis*. Springer, New York, 1989. Zbl 0665.47038, MR0987431.

[18] P. Krejčí. *Hysteresis, Convexity and Dissipation in Hyperbolic Equations*. Gakkotosho, Tokyo, 1996. Zbl 1187.35003, MR2466538.

[19] P. Krejčí, J. P. O'Kane, A. Pokrovskii, and D. Rachinskii. Stability results for a soil model with singular hysteretic hydrology. *Journal of Physics: Conference Series*, 268(1):012016, 2011. DOI 10.1088/1742-6596/268/1/012016.

[20] P. Krejčí, J. P. O'Kane, A. Pokrovskii, and D. Rachinskii. Properties of solutions to a class of differential models incorporating Preisach hysteresis operator. *Physica D: Nonlinear Phenomena*, 241(22):2010–2028, 2012. MR2994340, DOI 10.1016/j.physd.2011.05.005.

[21] Pavel Krejčí. On Maxwell equations with the Preisach hysteresis operator: the one-dimensional time-periodic case. *Appl. Math.*, 34:364–374, 1989. Zbl 0701.35098, MR1014077.

[22] Pavel Krejčí. Resonance in Preisach systems. *Appl. Math.*, 45:439–468, 2000. Zbl 1010.34038, MR1800964, DOI 10.1023/A:1022333500777.

[23] Pavel Krejčí and Klaus Kuhnen. Compensation of complex hysteresis and creep effects in piezoelectrical actuated systems - a new Preisach modeling approach. *IEEE Transactions on Automatic Control*, 54(3):537–550, 2009. MR2191546, DOI 10.1109/TAC.2009.2012984.

[24] I. Mayergoyz. *Mathematical Models of Hysteresis and Their Applications*. Elsevier, 2003. Zbl 0723.73003, MR1083150.

[25] Isaak Mayergoyz and Giorgio Bertotti, editors. *The Science of Hysteresis, 3-volume set*. Elsevier, Academic Press, 2005. Zbl 1142.34028, MR2307931.

[26] S. McCarthy and D. Rachinskii. Dynamics of systems with Preisach memory near equilibria. *Mathematica Bohemica*, page accepted.

[27] A. Pimenov and D. Rachinskii. Linear stability analysis of systems with Preisach memory. *Discrete and Continuous Dynamical Systems - Series B*, 11(4):997–1018, 2009. Zbl 1181.47075, MR2505656, DOI 10.3934/dcdsb.2009.11.997.

[28] Alexander Pimenov, Tom C. Kelly, Andrei Korobeinikov, Michael J.A. O'Callaghan, Alexei V. Pokrovskii, and Dmitrii Rachinskii. Memory effects in population dynamics: Spread of infectious disease as a case study. *Mathematical Modelling of Natural Phenomena*, 7:204–226, 2012. Zbl 06074655, MR2928740, DOI 10.1051/mmnp/20127313.

[29] A. Visintin. *Differential Models of Hysteresis*. Springer, Berlin, 1994. MR1329094.

[30] C. Visone. Hysteresis modelling and compensation for smart sensors and actuators. *Journal of Physics: Conference Series*, 138:012028, 2008. DOI 10.1088/1742-6596/138/1/012028.